

Theory of the Hylan Hadron Hose

R. H. Milburn
Tufts University
Medford, MA 02155

ABSTRACT

We present some analytical solutions to describe charged particle trajectories in the 800 m NuMI decay region in the presence of the circular magnetic field of a long straight wire carrying a given current parallel to the tunnel axis. This analysis may prove illuminating to the interpretation of phenomena in Hylan's ingenious scheme for additional focussing of the decaying hadron ensemble.

1. Introduction

Jim Hylan has made the clever proposal that a long current-carrying wire run down the axis of the 800 m NuMI decay pipe might provide sufficient focussing of the positively charged ensemble of decaying hadrons to keep them away from the pipe walls and thus reduce the neutron generation of ground water tritium and similar nuisances.¹ This scheme might also ameliorate the systematic off-axis displacements caused by the geomagnetic field.^{2,3} He has made a number of GEANT-based simulation studies to verify the feasibility of his ideas, with tantalizing results suggesting that the scheme may not only be beneficial to the problems indicated above but might also produce distinct improvements in the wide-band neutrino beam (WBB) spectra, both far- and near-field. Wes Smart has also studied the scheme, using the PBEAM Monte Carlo.

It has since become apparent that what Hylan has, in fact, independently reinvented is a beam transport system described more than one-third of a century ago by S. van der Meer.⁴ The latter's analysis, in turn, stems from still earlier papers, including one which is concerned with focussing by plasma currents.^{5,6} Van der Meer's report itself concentrated upon a possible use of his "Beam Guide" to extract and transport high intensity secondary beams from internal accelerator targets, and thus carried through a detailed analysis of features such as acceptances and steering capabilities. He also addressed some of the electrical and energetic practicalities relevant

to building a functioning system. He further notes the similarity of the theory to that for his earlier contribution to neutrino physics, the magnetic horn!⁷ In a subsequent CERN report Regenstreif presented an exhaustive and highly geometrical analysis of the orbits in and acceptances of “Beam Guides,” along similar lines to those of van der Meer.⁸ Regenstreif also noted, in passing in his Introduction, that such a system might be used (as Hlyen proposes) to concentrate a beam of pions over a few hundred meters so that they can decay in flight to generate neutrinos. It will be challenging to see whether NuMI can now put this imaginative Phoenix to good practical use!

The NuMI beam generation process is very complex, from the proton interactions in the primary target through the complex transport and decay pipe systems, all of which are subject to various mechanical perturbations and electromagnetic uncertainties. Detailed Monte Carlo procedures are consequently essential to achieving the precision understanding of the near- and far-field neutrino spectra required for the MINOS oscillation studies, and for understanding how to monitor and control the beam to achieve stability, as well as public credibility, for these spectra.

The following report is aimed at achieving a sufficient theoretical understanding of the “hadron hose” (as we shall continue to denote the NuMI reincarnation) so that the precision of the several Monte Carlo procedures may be verified with confidence as they track hadrons along their often rather complicated helicoid trajectories in the vicinity of the nearly-singular magnetic fields at the current-carrying wire. The basic calculations must obviously retrace much the same analytical ground as those in the earlier studies of van der Meer and Regenstreif, but our present thrust is aimed at the generation of trajectory data having parameters more appropriate to the NuMI application. In doing this we can also use powerful modern interactive computing resources not available at the time to the pioneering workers at CERN. I have also tried, in the following, to develop an analysis which has some didactic virtues, this with the hope that a clear presentation of the physics involved in hadron hose phenomena might enhance the creative appreciation of their possible effects in the very complex NuMI beam environment.

2. Coordinate Systems & Equations of Motion

For the following calculations we shall use a right-handed coordinate system almost, *but not quite*, identical to that based upon the nominal central beam line extending from Fermilab to the MINOS far detector at Soudan. The difference is that the axis along the beam tunnel is to be defined by the long, straight, current-carrying wire, which may not be quite parallel to the beam axis, and which may also be displaced from it laterally. Thus we shall use:⁹

- z-axis : the long straight wire carrying a (positive) current, I ,
- x-axis : in the plane containing the z-axis and the upward vertical,
- y-axis : \perp x- and z-axes, completing a right-handed (xyz) triad.

As usual, we define the set of unit vectors $(\hat{i}, \hat{j}, \hat{k})$ parallel to the (x,y,z) axes, respectively.

We start with the textbook calculation of particle motion in a uniform, static magnetic field as presented by Jackson.¹⁰ The velocity \mathbf{v} of a relativistic particle of mass, m , and positive charge, e , travelling in a uniform, static, magnetic induction, \mathbf{B} is given by

$$\frac{d\mathbf{v}}{dt} = \mathbf{v} \times \omega_{\mathbf{B}}, \quad (1)$$

where the gyration frequency is, for constant total particle energy E , in gaussian units,

$$\omega_{\mathbf{B}} = \frac{e\mathbf{B}}{\gamma mc} = \frac{ec\mathbf{B}}{E}. \quad (2)$$

It is convenient to parametrize the time variable in terms of the curvilinear coordinate, $s = \beta ct$, measured along the trajectory. Since the magnetic field does not affect the particle energy the velocity parameter β is a constant. In practice for NuMI, $s \doteq z$, but use of s yields simpler, more exact, results. We find, then, that the velocity vector $\mathbf{v}(s)$ satisfies

$$\frac{d\mathbf{v}}{ds} = \frac{1}{R_0} \mathbf{v} \times \hat{\mathbf{b}}, \quad (3)$$

where the unit vector

$$\hat{\mathbf{b}} = \frac{\mathbf{B}}{B} \quad (4)$$

and the gyration radius

$$R_0 = \frac{pc}{eB}. \quad (5)$$

Note that Eqn. 3 is homogeneous in the distance units for s and R_0 , and that the velocity $\mathbf{v}(s)$, expressed in terms of slopes, is dimensionless.

The curvature parameter R_0 is related to the field B and momentum p by the familiar practical formula

$$p [\text{GeV}/c] = 0.2997\dots B[\text{T}] R_0[\text{m}], \quad (6)$$

and the field itself, $B[\text{T}]$ at distance $r[\text{m}]$ from a long straight current $I[\text{A}]$, is of magnitude given by Ampere's Law (in SI units),

$$B = \frac{\mu_0 I}{2\pi r}, \quad (7)$$

where $\mu_0 = 4\pi \cdot 10^{-7}$. Thus we can write

$$R_0 = \frac{r}{K} \quad (8)$$

where the dimensionless field-strength parameter K may be calculated from

$$K = \frac{0.6 \times 10^{-7} I[\text{A}]}{p[\text{GeV}/c]}. \quad (9)$$

Thus the equation of motion Eqn. 3 becomes

$$\frac{d\mathbf{v}}{ds} = \frac{K}{r} \mathbf{v} \times \hat{\mathbf{b}}. \quad (10)$$

Since the magnetic field is everywhere tangent to circles concentric with the current, it is natural to introduce a cylindrical polar coordinate system (r, θ, z) by letting $x = r \cos \theta$, $y = r \sin \theta$, $z = z$. Representing the unit orthonormal triad for this basis by $(\hat{u}_r, \hat{u}_\theta, \hat{u}_z)$, we note that our unit field vector $\hat{b} = \hat{u}_\theta$. The velocity vector becomes $\mathbf{v} = v_r \hat{u}_r + v_\theta \hat{u}_\theta + v_z \hat{u}_z$ from which we can convert Eqns. 10 to the cylindrical form

$$\begin{aligned} \frac{dv_r}{ds} - v_\theta \left(\frac{d\theta}{ds} \right) &= - \left(\frac{K}{r} \right) v_z, \\ \frac{dv_\theta}{ds} + v_r \left(\frac{d\theta}{ds} \right) &= 0, \\ \frac{dv_z}{ds} &= \left(\frac{K}{r} \right) v_r. \end{aligned} \quad (11)$$

Noting further that $\mathbf{r} = r \hat{u}_r + z \hat{u}_z$, where $\mathbf{v} = d\mathbf{r}/ds$, we obtain finally the exact trajectory equations

$$\begin{aligned} \frac{d^2 r}{ds^2} - r \left(\frac{d\theta}{ds} \right)^2 &= - \left(\frac{K}{r} \right) v_z, \\ r \frac{d^2 \theta}{ds^2} + 2 \left(\frac{dr}{ds} \right) \left(\frac{d\theta}{ds} \right) &= 0, \\ \frac{d^2 z}{ds^2} &= \left(\frac{K}{r} \right) v_r. \end{aligned} \quad (12)$$

The θ -equation, above, may be solved directly in terms of the angular velocity function $\omega(s) = d\theta/ds$ since it becomes

$$d\omega = -2\omega \frac{1}{r} dr \quad (13)$$

whose solution is

$$\omega r^2 = C, \quad (14)$$

where C is a constant. This simply shows the constancy of the particle's z -component of angular momentum (per unit mass) which is left invariant by the simple circular field geometry.

Suppose that the particle enters the decay pipe at coordinate s (or z) = 0 at a distance r_0 off-axis and with the θ -component of its slope $v_\theta = r_0 \omega_0$. Then, along the subsequent trajectory

$$\left(\frac{\omega}{\omega_0} \right) = \left(\frac{r_0}{r} \right)^2. \quad (15)$$

The radial member of Eqns. 12 becomes

$$\frac{d^2 r}{ds^2} = - \left(\frac{K}{r} \right) v_z, + \left(\frac{L^2}{r^3} \right), \quad (16)$$

where the initial and constant axial angular momentum component is $L = r_0^2 \omega_0$.

We note that the term $v_z = (dz/ds) \doteq 1$ and so rewrite the above, alternatively and slightly approximately, as

$$\frac{d^2 r}{ds^2} = - \frac{K}{r} \left[1 - \left(\frac{L^2}{K} \right) \frac{1}{r^2} \right], \quad (17)$$

Of the two dimensionless parameters in this last equation, \sqrt{K} simply scales the ratio of the radial distances to the longitudinal, and L^2/K characterizes an effective “angular momentum potential barrier” which will keep certain particles away from the axis — where they might otherwise damage the current-carrying conductor! We shall see that this barrier can be significant under the conditions which obtain for the NuMI beam and decay tunnel.

The following section will be devoted to efforts to solve Eqn. 17.

3. Reduction to Scaled Equation

It is helpful to scale the problem into a form which reveals its essential features. First, we scale the longitudinal (z) dimensions by defining $u \equiv \sqrt{K}s$. Then Eqn. 17 becomes

$$\frac{d^2 r}{du^2} = - \frac{1}{r} \left[1 - \left(\frac{L^2}{K} \right) \frac{1}{r^2} \right]. \quad (18)$$

This easily yields to a first integration, giving

$$\left(\frac{dr}{du} \right)^2 = 2 \ln \left(\frac{1}{r} \right) - \left(\frac{L^2}{K} \right) \frac{1}{r^2} + \mathcal{C}. \quad (19)$$

We now assume that the trajectory being represented begins (at $z = z_0$) at a radius r_0 from the z -axis and that it has a slope relative to the z -direction ($d\mathbf{v}/ds = \sqrt{K}d\mathbf{v}/du$) whose magnitude is represented by

$$r'_0 \equiv \left| \frac{d\mathbf{v}}{ds} \right| \quad (20)$$

and whose direction projected on the $x - y$ plane makes an angle ψ_0 with respect to the r -direction. Thus $v_r = r'_0 \cos \psi_0$ and $v_\theta = r'_0 \sin \psi_0$. The constant z -component of angular momentum, L , is then given by $L = r_0 r'_0 \sin \psi_0$. With this initial condition Eqn. 19 becomes

$$\left(\frac{dr}{du} \right)^2 = 2 \ln \left(\frac{r_0}{r} \right) + \left(\frac{r'^2_0}{K} \right) \cdot \left[1 - (\sin^2 \psi_0) \left(\frac{r_0}{r} \right)^2 \right]. \quad (21)$$

Three final scaling definitions,

$$\rho \equiv \frac{r}{r_0} \geq 0, \quad (22)$$

$$w \equiv \frac{u}{r_0} = \left(\frac{\sqrt{K}}{r_0} \right) \cdot s \quad (23)$$

and

$$\beta_0^2 \equiv \frac{(r'_0)^2}{K}, \quad (24)$$

lead to the ultimate exact dimensionless first integral of the radial motion equation,

$$\left(\frac{d\rho}{dw} \right)^2 = 2 \ln \left(\frac{1}{\rho} \right) + \beta_0^2 \cdot \left[1 - \frac{1}{\rho^2} \sin^2 \psi_0 \right]. \quad (25)$$

There are only two relevant dimensionless constants: β_0^2 which characterizes the magnitude of the entering trajectory slope, relative to the effective curvature induced by the magnetic field, and ψ_0 which describes the amount of angular momentum present, which must be conserved.

Before proceeding to examine a variety of special cases, it will be useful to estimate the magnitude of the various critical parameters, including β_0^2 , for typical NuMI trajectories. We refer to Eqn. 9 and establish several special cases, all assuming a typical wire current of $I = 6000\text{A}$.

- *Case s* (soft hadrons : 6 GeV/c with typical entering radius $r_0 = 30$ cm and slope $r'_0 = 2$ mrad.)
- *Case h* (hard hadrons : 60 GeV/c with typical entering radius $r_0 = 30$ cm and slope $r'_0 = 1$ mrad.)
- *Case p* (protons : 120 GeV/c with typical entering radius $r_0 = 3$ cm. – assuming the wire is not quite on the beam axis – and slope $r'_0 = 0.1$ mrad.)

Thus the range of typical scaling parameters is typified by

$$\begin{aligned} \beta_{0s}^2 &= 0.067 \\ \beta_{0s} &= 0.259 \\ r_{0s} &= 0.3 \text{ m}, \\ (1/\sqrt{K})_s &= 129 \\ K_s &= 0.00006 \end{aligned}$$

$$\begin{aligned} \beta_{0h}^2 &= 0.167 \\ \beta_{0h} &= 0.4086 \end{aligned}$$

$$\begin{aligned}
r_{0h} &= 0.3 \text{ m}, \\
(1/\sqrt{K})_h &= 408 \\
K_h &= 0.000006 \\
\\
\beta_{0p}^2 &= 0.003 \\
\beta_{0p} &= 0.0548 \\
r_{0p} &= 0.03 \text{ m} \\
(1/\sqrt{K})_p &= 577 \\
K_p &= 0.000003.
\end{aligned} \tag{26}$$

Here follow several illustrative situations in which one may draw simple conclusions in closed form without need for a tedious integration of Eqn. 25.

Purely radial motion : “no angular momentum”

This case occurs when $\psi_0 = 0$ or 180° . The trajectory’s entering slope will be brought parallel to the axis at a radius given by the condition

$$0 = -\ln \rho^2 + \beta_0^2, \tag{27}$$

which translates to

$$r = r_0 e^{\frac{\beta_0^2}{2}} = r_0 e^{\frac{(r'_0)^2}{2K}}. \tag{28}$$

From Eqns. 26 it is seen that typical divergent hadrons are brought to heel, parallel to the axis, within a further 20% of their entering radii.

We may establish simply, for this radial-only case, how far a particle must travel from the point where it has zero slope until it crosses the axis (and impacts the current-carrying wire). For this, let an initial radial slope, $r'_0 = 0$ occur at $w = 0$, so that $\beta_0^2 = 0$, and Eqn. 25 becomes

$$\left(\frac{d\rho}{dw}\right)^2 = -2\ln \rho \equiv 2\sigma^2. \tag{29}$$

This equation can be easily integrated explicitly over the slope parameter, σ , from the initial coordinate, $w = 0$, to a final coordinate, w_2 , where the slope must become $-\infty$. One finds

$$w_2 = \sqrt{2} \cdot \int_{-\infty}^0 d\sigma e^{-\sigma^2} = \sqrt{\frac{\pi}{2}}. \tag{30}$$

Thus an effective focal length, in terms of the maximal radius r_+ at which it was travelling parallel to the axis, may be found by removing the scaling,

$$f = \left(\frac{r_+}{\sqrt{K}}\right) \cdot \sqrt{\frac{\pi}{2}}. \tag{31}$$

This is proportional to r_+ , as might be expected from the $1/r$ field dependence. Using the scaling examples of Eqns. 26 and taking $r_+ \approx r_0$ we find typical focal lengths to be, for the three cases,

$$\begin{aligned} f_s &= 48.5 \text{ m}, \\ f_h &= 153.4 \text{ m}, \\ f_p &= 21.7 \text{ m}. \end{aligned} \tag{32}$$

Thus the (s,h,p) particles would typically execute (purely) radial oscillations along the decay tunnel with respective periods (97, 307, 44) meters.

Radial oscillation with “angular momentum” present

If the initial trajectory has a θ -component of velocity, one can still infer from Eqn. 25 the range of radial motion by finding its roots, that is, the values of ρ for which the radial component of slope vanishes. This is equivalent to letting $\psi_0 = 90^\circ, 270^\circ$ at an initial location, which we shall take as the location of the maximum radius, r_+ . The initial slope parameter is thus purely tangential, $(\beta_0 \sin \psi_0)^2 \equiv \beta_+^2$, and Eqn. 25 becomes

$$0 = \ln \left(\frac{1}{\rho^2} \right) + \beta_+^2 \cdot \left[1 - \frac{1}{\rho^2} \right]. \tag{33}$$

One root of this is obviously, as it must be, $\rho = 1$. The other, for the minimum radius r_- defined by $\rho_- = r_-/r_+ \leq 1$, must be found by solving Eqn. 33 numerically for given β_+^2 . We easily calculate some typical values of β_+^2 as a function of ρ , as shown in Table 1.

Thus, for the largest-slope “h” case (hard hadrons), if purely azimuthal, the minimum radius is about one-fifth of the maximum. For the “s” (soft) hadron case the fraction is one-tenth, and for the “p” (proton) case it is about 0.02. Thus such protons starting from a radius 3 cm away from the wire axis will approach to a radius of only 0.6 mm. It should be remembered that this is for protons whose slopes are already purely azimuthal; protons with some outward radial slope will reach their maximum r_+ at somewhat larger radii than 3 cm, but even these will be subsequently be brought in very close to the wire axis. [To avoid burning out this wire it might be wise to impose an even larger and compulsory “angular momentum” on the proton beam by skewing the wire with respect to the latter’s axis!]

This calculation of the effective envelope of the radial oscillations of the particle trajectories does not in itself yield the longitudinal scale of the phenomenon. While it may be expected to be comparable to that found explicitly in the “zero-angular momentum” cases of Eqns. 32, a more precise determination requires the full solution of the equations of motion, which follows.

Table 1: Radial Range (scaled) for various “Angular Momenta”.

| β_+^2 | ρ | β_+^2 | ρ | β_+^2 | ρ |
|-------------|--------|-------------|--------|-------------|--------|
| 1.0000 | 1.0000 | 0.8893 | 0.8912 | 0.7396 | 0.7499 |
| 0.6092 | 0.6310 | 0.4970 | 0.5309 | 0.4018 | 0.4467 |
| 0.2985 | 0.3548 | 0.2186 | 0.2818 | 0.1715 | 0.2371 |
| 0.1670 | 0.2328 | 0.1337 | 0.1995 | 0.1035 | 0.1679 |
| 0.0797 | 0.1413 | 0.0670 | 0.1262 | 0.0667 | 0.1259 |
| 0.0510 | 0.1059 | 0.0465 | 0.1000 | 0.0353 | 0.0841 |
| 0.0267 | 0.0708 | 0.0151 | 0.0501 | 0.0102 | 0.0398 |
| 0.0057 | 0.0282 | 0.0030 | 0.0195 | 0.0019 | 0.0150 |
| 0.0009 | 0.0100 | 0.0003 | 0.0054 | 0.0000 | 0.0000 |

4. Full Radial and Angular Solution

The full solution of the trajectory problem appears to require the numerical solution of the system Eqns. 12. To simplify the process it is convenient to reduce them to a scaled and dimensionless form, using an extension of the earlier definitions, to wit:

$$\begin{aligned}
 \rho &\equiv \frac{r}{r_0} \geq 0, \\
 s &\equiv \left(\frac{r_0}{\sqrt{K}} \right) w, \\
 z &\equiv \left(\frac{r_0}{\sqrt{K}} \right) \xi.
 \end{aligned} \tag{34}$$

Note that $d\xi/dw = dz/ds \doteq 1$ for our application.

The scaled forms of Eqns. 12 are thus the set of equations, still exact,

$$\begin{aligned}
 \frac{d^2 \rho}{dw^2} - \rho \left(\frac{d\theta}{dw} \right)^2 &= - \left(\frac{1}{\rho} \right) \left(\frac{d\xi}{dw} \right), \\
 \rho \frac{d^2 \theta}{dw^2} + 2 \left(\frac{d\rho}{dw} \right) \left(\frac{d\theta}{dw} \right) &= 0, \\
 \frac{d^2 \xi}{dw^2} &= \left(\frac{K}{\rho} \right) \left(\frac{d\rho}{dw} \right).
 \end{aligned} \tag{35}$$

The second of these can easily be integrated, as before, to yield the constancy of the scaled longitudinal “angular momentum” component, $\rho^2(d\theta/dw)$.

Further analysis will be based upon the practical requirements of the software package, MAPLE, as installed on a Pentium-Pro 200 MHz personal computer.¹¹ Among the routines of this package is one which performs a Runge–Kutta integration of a set of coupled first–order differential equations whose members are of the form:

$$\left(\frac{dx_i}{dt}\right) = f_i(t, x_1, x_2, x_3, \dots, x_n), i = 1, \dots, n, \quad (36)$$

where t is the common argument of the set of solution functions $\{x_i(t)\}$.

Equations 35, above, may be written in this form using the variables (w, ρ, θ, ξ) and their slopes relative to w , (ρ', θ', ξ') . Thus,

$$\begin{aligned} \frac{d\rho}{dw} &= \rho', \\ \frac{d\theta}{dw} &= \theta', \\ \frac{d\xi}{dw} &= \xi', \\ \frac{d\rho'}{dw} &= -\left(\frac{1}{\rho}\right) \xi' + \rho (\theta')^2, \\ \frac{d\theta'}{dw} &= -\left(\frac{2}{\rho}\right) \rho' \theta', \\ \frac{d\xi'}{dw} &= \left(\frac{K}{\rho}\right) \rho'. \end{aligned} \quad (37)$$

These must then be integrated numerically, propagating in the beam–line parameter, w , from the initial conditions $(w_0, \rho_0, \rho'_0, \theta_0, \theta'_0, \xi_0, \xi'_0)$.

One may note, in passing, that the last of these equations may be integrated directly to yield the equation $\xi' = \ln(\rho^K) + \text{constant}$. Since K is typically $O(10^{-4})$ or smaller, the approximate equivalence of variables (ξ, w) , and (z, s) , may be demonstrated quantitatively.

A typical integration of Eq. 37 is illustrated in Fig. 1. This is for the “s” (soft hadron) case and shows the oscillations between the maximum and minimum radial coordinates of the particle – as a fraction of the former – plotted against the scaled longitudinal parameter, w , over a long range including many cycles. A more precise plot would show some small fluctuations in the apparent maximum and minimum amplitudes which are artifacts from the use of a finite set of plotting points. In addition, however, one must be careful to use a sufficiently fine-grained longitudinal mesh in the basic Runge–Kutta calculations to handle the quasi-cusp conditions at small radii, near the wire. This is especially true for the “p” case, which simulates the primary proton beam.

The angular circulation of the soft “s” hadrons shown in Fig. 1 may be illustrated by plotting the transverse variables y -versus- x , as is done in Fig. 2. The angular

periodicity is clearly different from that of the radial parameter, ρ . In both of these plots the points are equally spaced in the longitudinal w -variable, and thus represent constant increments in time.

The preceding plots for each of the illustrative cases, [“h”, “s”, “p”], are presented together for comparison in Fig. 3. Only a few radial cycles are included for each – to reduce confusion, and also to yield adequate precision at small radii in the “p” case, at the bottom of the figure. Qualitatively, the three trajectories are all quite similar.

5. Conclusion

It is obvious that the detailed design of a beam system using the Hadron Hose *cum* Beam Guide concept requires much more than a simple analytic solution of the motion equations for a few idealized cases. This is particularly true when the ultimate beam in question is of secondary neutrinos generated at random points along an extended ensemble of hadron trajectories, and is strongly dependent upon the exact direction of the hadronic momentum vector at the point of decay. In short, full-scale Monte Carlo analyses, such as based on PBEAM and/or GEANT, are imperative for practical work. However, it is important for the latter forms of analysis to have some independent cross-checks on the precision of the Monte Carlo tracking algorithms, especially when dealing with strongly non-uniform magnetic fields such as occur near the current-carrying wire used in the Hose. It is hoped that the preceding “hose theory” development, and the accompanying tables and figures, can provide some cross checks, as well as help to develop for the user an intuitive appreciation of the behavior of particles traversing this quite elegant beam system.

One should conclude this report with a salute to Jim Hylan for conceiving the hose as a possible solution to a host of NuMI beam problems, and to S. van der Meer who had already worked out so much of this material over a third of a century ago.

6. Acknowledgments

I am very grateful to Jim Hylan for the early revelation of his hadron hose concept, and to Jim, Wes Smart and their Fermilab colleagues for their support and encouragement of my nibbling at a number of the more exciting questions emerging from their impressive body of work toward development of the Fermilab NuMI neutrino beam.

References

1. James Hylan (private communication, Nov. 21, 1996)
2. *The NuMI Neutrino Beam and Geomagnetism*, R.H. Milburn, Note NuMI-B-188, June 28, 1996.
3. *The Geomagnetic Distortion of the NuMI Neutrino Beam*, R.H. Milburn, Note NuMI-B-226, November 19, 1996.
4. *The beam guide, a device for the transport of charged particles*, S. van der Meer, CERN 62-16, April 17, 1962.

5. *Motion of a relativistic charged particle in the magnetic field produced by a constant cylindrical current of a rarefied plasma*, N.I. Stepa, Soviet Physics – Techn. Physics, **4**, 1237 (1960).
6. *Die bewegung geladener Teilchen im Magnetfeld eines geraden stromdurchflossenen Drahten*, Zeitsch. f. Naturf. **14A**, 47, (1959).
7. *A directive device for charged particles and its use in an enhanced neutrino beam*, CERN 61-7.
8. *Contributions to the theory of the Beam Guide*, CERN 64-41, E. Regenstreif, September 24, 1964.
9. The NuMI reader should be reminded that the present NuMI convention is to have the y -axis *upward* and the x -axis *westward*. Thus the coordinates used in this paper must be transformed by the 90° rotation ($x \rightarrow y, y \rightarrow -x$) to obtain NuMI beam coordinates.
10. *Classical Electrodynamics*, J.D. Jackson, Second Edition, Wiley, N.Y. p.581.
11. *MAPLE V, Release 3, Student Edition, 1995*. Brooks/Cole Publishing Co., 511 Forest Lodge Road, Pacific Grove, CA 93950 USA.

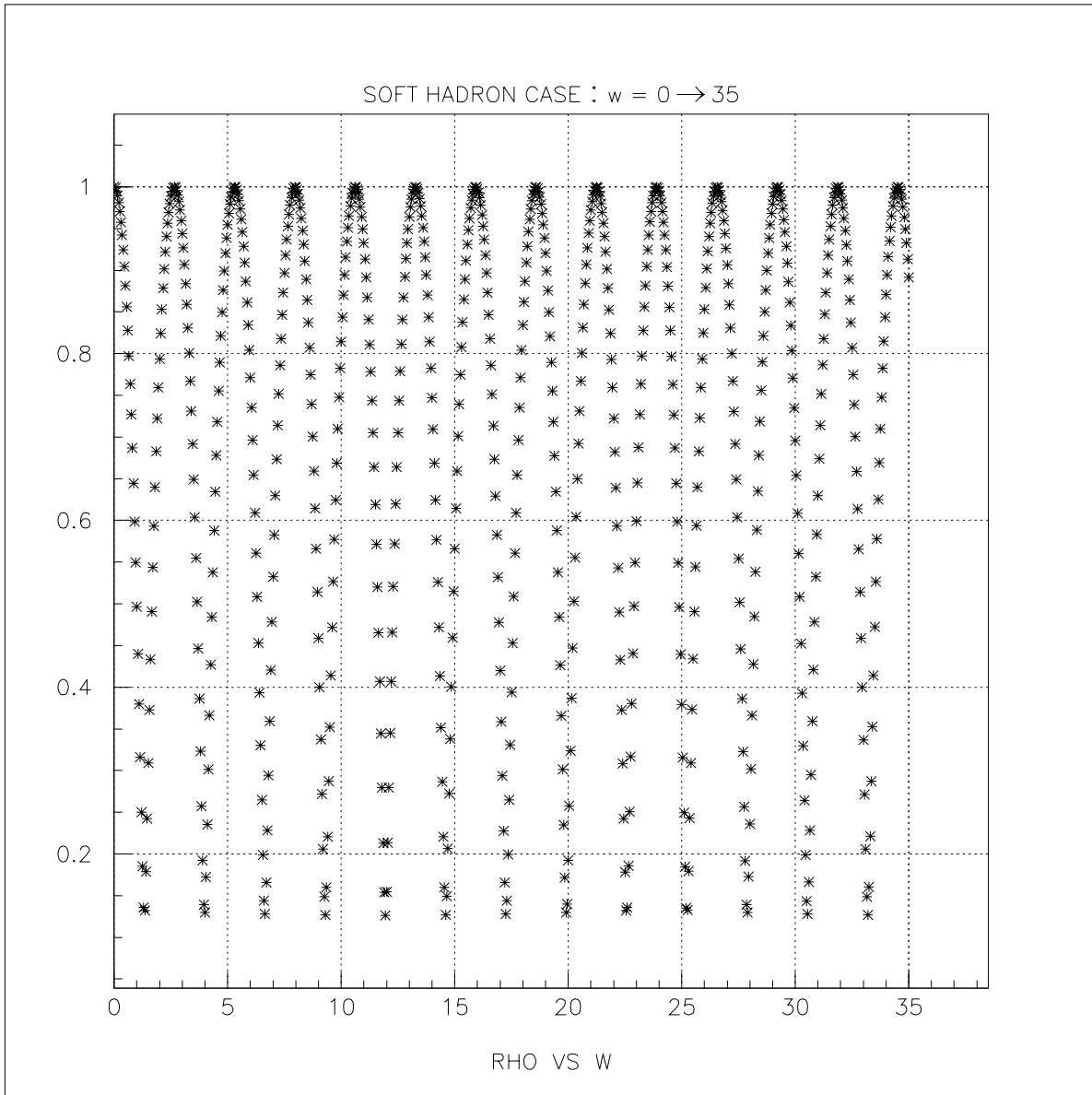


Figure 1: Plot of ρ vs w for the “s” (soft hadron) case, showing the oscillations between a maximum radius of 30 cm and a minimum of 4 cm.

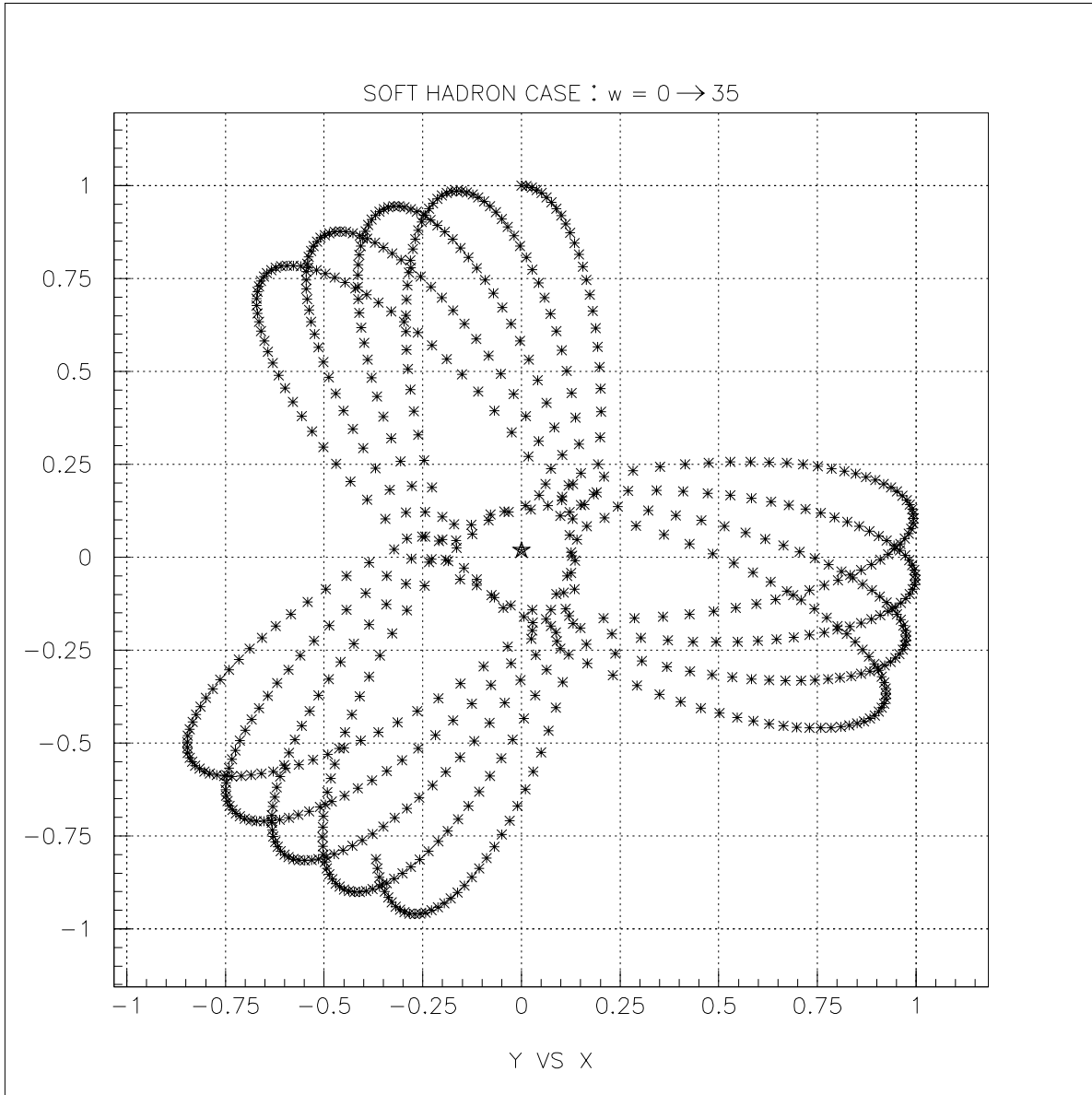


Figure 2: Plot of y vs x for the “s” (soft hadron) case, showing the trajectory circulation about the wire axis, indicated by a star, after starting from the point $[0, 1]$ at the top of the figure.

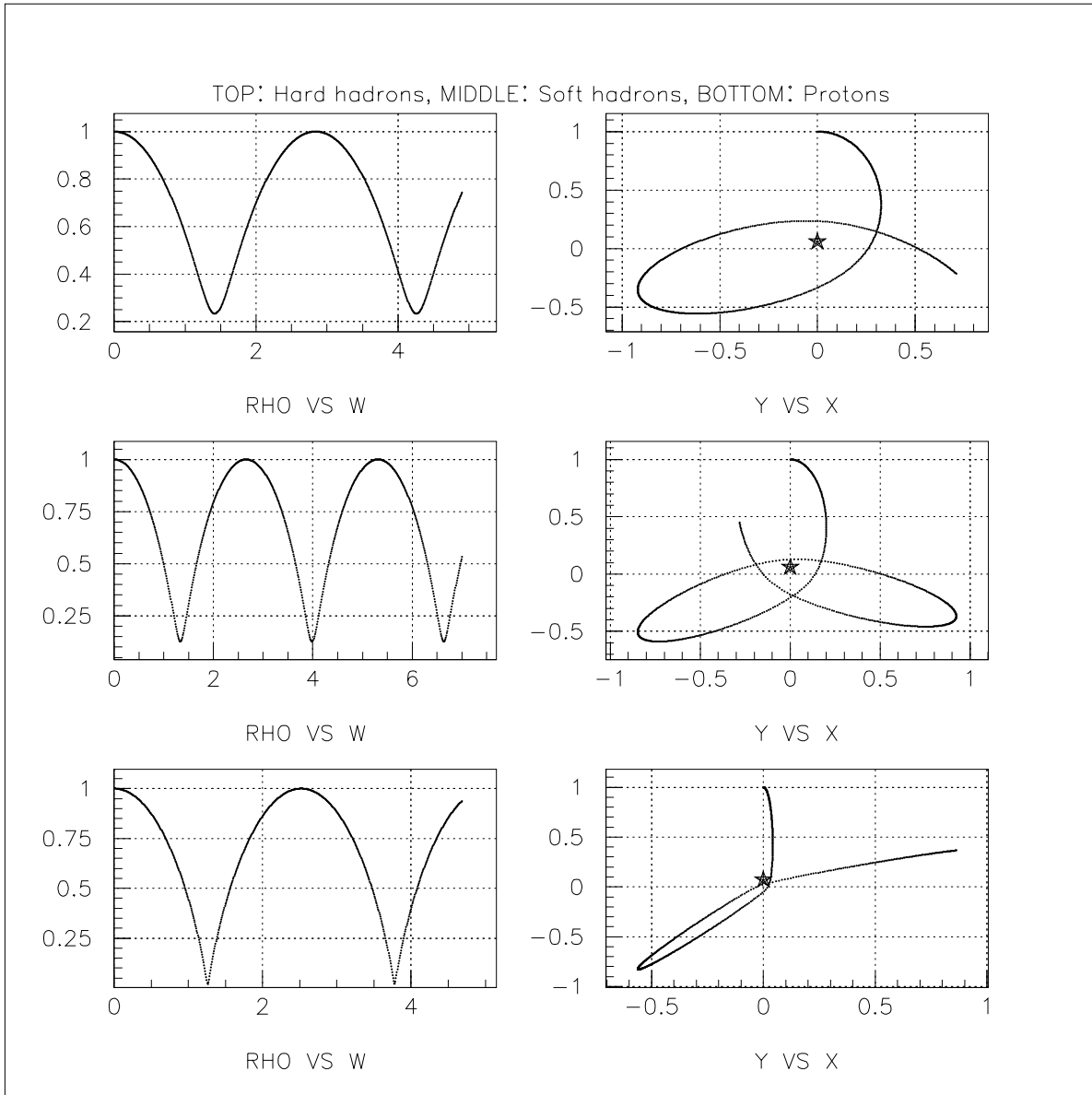


Figure 3: Comparison of Plots of ρ vs w and of y vs x for the “h” case (top), “s” case (middle) and “p” case (bottom) for the respective trajectories starting at the point $[0, 1]$ at the top of the right-hand figure set.